ISSN 0208-7774 TRIBOLOGIA 4/2019 p. 23–31
DOI: 10.5604/01.3001.0013.5962

Marzena LACHOWICZ*

CORROSIVE WEAR OF THE SELECTED TOOL STEELS

ZUŻYWANIE KOROZYJNE WYBRANYCH STALI NARZĘDZIOWYCH

Key words: tool steels, microstructure, carbides, corrosion, metallography, SEM.

Abstract: Wear is associated with processes leading to the gradual destruction of components, including the impact of physicochemical factors. Determining the relationship between microstructure and working properties of tool steels, including corrosion resistance, has significant importance to the preventing accelerated destruction of tools made of them. The purpose of the tests presented in this paper was to determine the resistance of selected tool steels to corrosion wear. To this end, electrochemical tests and a salt chamber test were carried out. Scanning electron microscope observations carried out after corrosion tests and combined with the earlier microstructural characteristics of the tested materials allowed the accessment of the impact of their microstructure and a clarification of the role of carbides in the development of corrosion.

Słowa kluczowe: stale narzędziowe, mikrostruktura, węgliki, korozja, metalografia, SEM.

Streszczenie: Zużywanie związane jest z procesami prowadzącymi do stopniowego niszczenia elementów, w tym również oddziaływaniem czynników o charakterze fizykochemicznym. Ustalenie zależności pomiędzy mikrostrukturą a własnościami użytkowymi stali narzędziowych, w tym odporności korozyjnej, ma istotne znaczenie w zapobieganiu przyśpieszonemu niszczeniu narzędzi z nich wykonanych. Celem przedstawionych w pracy badań było określenie odporności na zużycie korozyjne wybranych stali narzędziowych. W tym celu przeprowadzono badania elektrochemiczne oraz test w komorze solnej. Obserwacje mikroskopowe SEM zrealizowane po badaniach korozyjnych połączone z wcześniejszą charakterystyką mikrostrukturalną badanych materiałów pozwoliły na ocenę wpływu ich mikrostruktury i roli węglików w rozwoju korozji.

INTRODUCTION

Tool steels consist of a large group of unalloyed and alloyed steels that are used in the formation of other engineering materials. One of the essential requirements for tool steels is the durability of the tool shape. It is expected that the material from which it is made will exhibit good resistance to wear, which should be considered as all processes related to gradual destruction caused by various factors, including physicochemical factors. Usually, the impacts of a given type of wear process arise from a combination of various impacts. For example, corrosive wear often accompanies the mechanical wear of a freshly exposed metal surface, which should be considered as mechanical-corrosive wear (tribocorrosion) **[L. 1–8]**.

Usually, one of the factors causing wear is the leading one. Identification of the nature of elementary tool wear processes allows forecasting the working lifetime of tools, as well as preventing their accelerated destruction. Symptoms of tool wear can be the deterioration of the surface condition of the tool's working part, and changes in its shape and geometry. The progressing tool wear causes material loss in the surface layer. The intensity and state of wear leads to quantitative and qualitative changes in the characteristics of the workpiece's condition. Tool wear may lead to the deterioration of the surface quality of the workpiece as well as the accuracy of its dimensions and shape. However, the lifetime of tools is negatively affected by the intensity of working conditions, but also by the corrosivity of their working environment. The wear of cutting tools is closely related

* ORCID: 0000-0002-4959-2970. Wrocław University of Science and Technology, Faculty of Mechanical Engineering, I. Łukasiewicza 5 Street, 50-371 Wrocław, Poland.

to oxidation occurring as a result of high temperatures. We should also remember that when the tool is not in use, it is also exposed to electrochemical corrosion, especially in environments with high humidity. This leads to changes in the physicochemical properties of the surface as well as to the mechanical properties of the tool material. Corrosive wear is usually not a major cause of excessive tool steel wear, but tribological wear can be continued by the exposed steel surface as a result of rupture of its corrosion film by the workpiece **[L. 9]**. For this reason, the corrosion resistance of the tool's surface is an important factor influencing the stability of its shape. The tendency to corrode will determine the durability of the tool and the intensity of its wear processes. Materials that are heavily exposed to a corrosive environment are materials used as cutting tools of wood. The water and water-soluble components in the wood result in an electrochemical mechanism of corrosion **[L. 5–8]**. Similar risks apply to tools used in the food industry **[L. 2**, **4]**.

The corrosion behaviour of unalloyed steels is widely known, which can be directly transferred to tool steels. However, alloy steels are a significant group of these materials, and their ultimate mechanical properties are determined by heat treatment, which consists of hardening and tempering. The corrosion mechanism in carbide-reinforced steels with carbon contents much higher than that in austenitic steel should be generally different. The microstructure of these steels is obtained during heat treatment by means of a compromise between the necessity to limit the primary austenite grain growth and the need to dissolve alloy carbides. The question arises: How does the presence of primary and secondary carbides in tool steels affects the development of corrosion? For this reason, determining the relationship between microstructure and working properties of tool steels, including corrosion resistance, has significant importance to the operational durability of tools made of them. Research presented in work **[L. 2]** indicates that higher hardness of martensitic steel promotes intensification of electrochemical processes in tribocorrosion conditions. The matrix sites next to Cr-rich carbides become a preferential site to localized corrosive attack **[L. 10–14]**. The tempered martensitic steels have significant sensitivity to hydrogen embrittlement associated with precipitation of carbides **[L. 15]**. The author's experience indicates an important role of carbide precipitations in the development of martensitic steel corrosion. Examples of such corrosive changes occurring over the areas of carbide precipitations are found in microscopic observations and shown in **Fig. 1**. In both cases, selective corrosion was observed along the boundaries of martensite platelets, in the areas where alloy carbides are formed during the tempering of these steels. These grades of steel are used, for example, in surgical instruments. Both elements presented have been subject to corrosion damage during operation in conditions of exposure to corrosive environments rich in chlorides.

In this study, two selected tool steels were researched. Microstructural observation and surface analysis were conducted to determine its correlation with corrosion behaviour. Tools subjected to significant changes in working surface temperature during its work cycle are vulnerable to surface changes of the microstructure **[L. 16]**. For this reason, the role of the microstructure in areas exposed to degradation changes caused by the fact of operation and its conditions is particularly important.

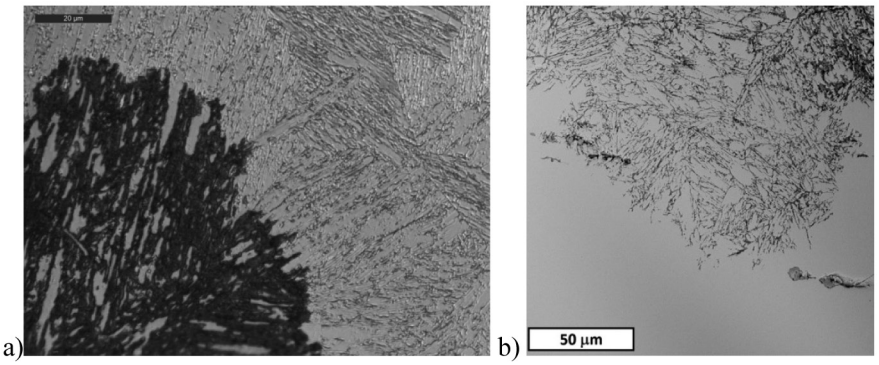

Fig. 1. Microscopic image of corrosion changes progressing in the areas of carbide precipitations in martensitic steel: a) X46Cr13 according to standard PN EN 10088. Light microscopy; b) X30Cr13 according to standard PN EN 10088. SEM

Rys. 1. Obraz mikroskopowy zmian korozyjnych postępujących po obszarach wydzieleń węglików w stali martenzytycznej: a) X46Cr13 zgodnej z normą PN EN 10088. Mikroskopia świetlna; b) X30Cr13 zgodnej z normą PN EN 10088. SEM

MATERIAL AND METHODOLOGY

The aim of the tests carried out was to determine the resistance of selected tool steels to corrosion wear in the operational layer at a tool standstill (without mechanical component). For this purpose, tool steels in the annealing state of delivery were used according to research hypothesis that martensitic steels exposed to the thermal exploitation can be tempered in the surface layer. As a consequence, conditions similar to the annealed state are obtained in this area.

Electrochemical tests were carried out using methods including the measurement of the open circuit potential E_{OCP} and recording the i = f(E) dependence during polarization tests in the three-electrode measurement system. The fully automated measurement system consisted of a measuring vessel, the ATLAS 0531 ELEKTROCHEMICAL UNIT&IMPEDANCE ANALYSER potentiometer, and a computer controller. The auxiliary electrode was made of austenitic steel, while a saturated Ag/AgCl electrode was used as a reference electrode. The samples for corrosion tests were abraded with emery paper up to 800 grit. The surface of the working electrode (sample) was 0.785 cm^2. The results were obtained based on three samples for each grade of material. Before starting the measurement, each sample was immersed for 20 min in a 5% NaCl solution at ambient temperature for stabilization, after which it was subjected to polarization in the same solution in the anodic direction with the scan rate of dE/dt = 1 mV/s. The corrosion solution used had the pH value of 7.4. The initial value of the potential was determined based on the stabilized value of the potential of the open circuit E_{OCP}, assuming a value lower by about 200 mV.

In order to determine the corrosion rate (CR) and to characterize changes occurring on the surface, a neutral salt spray test (NSS) was carried out in accordance with standard PN-EN ISO 9227. The chamber temperature during the test was 35 ±0.4°C, salt spray precipitation was 1.57 ml/h/80 cm^2, the pH of the corrosion solution was 6.9 and the conductivity of demineralised water amounted to 10 μS/cm. The test lasted for 96 h. The results were calculated based on three samples for each steel.

The chemical compositions of the steels used for the tests were determined using the optical emission spectrometry (GDOES) method using a LECO GDS500A analyser. They are summarized in **Tables 1** and **2**. They were compatible, respectively, with X153CrMoV12 (1.2379) cold work steel grades and X37CrMoV5-1 (1.2343) hot work steel grades, according to standard PN-EN ISO 4957. The first of them, according to withdrawn PN standards, was designated as NC11LV, while the second one is known under the term WCL.

Table 1. Chemical composition of the X153CrMoV12 cold work tool steel tested
Tabela 1. Skład chemiczny badanej stali narzędziowej do pracy na zimno gatunku X153CrMoV12

Element	C	Mn	Si	P	S	Cr	V	Mo	Ni
Content [wt%]	1.61	0.56	0.27	0.026	0.014	10.9	0.72	0.73	0.18

Table 2. Chemical composition of the X37CrMoV5-1 hot work tool steel tested
Tabela 2. Skład chemiczny badanej stali narzędziowej do pracy na gorąco gatunku X37CrMoV5-1

Element	C	Mn	Si	P	S	Cr	V	Mo	Ni
Content [wt%]	0.38	0.46	1.12	0.020	0.011	5.47	0.33	1.23	0.22

Microscopic examinations were carried out using a Leica DM 6000 M optical microscope and a Phenom World ProX scanning electron microscope equipped with an X-ray microanalyser. Hardness measurements were performed using a Zwick Roell ZHU 8187,5 LKV durometer. The X153CrMoV12 steel tested had the hardness of 252 ±9 HV3, while the X37CrMoV5-1 steel 220 ±3 HV3, respectively.

THE AUTHOR'S CURRENT RESEARCH

Microstructure of tested steels

The microstructure of the X153CrMoV12 cold work tool steel was typical of material subjected to soft annealing. The separation of primary carbides evenly distributed in the spheroidite matrix was observed (**Fig. 2**). The distribution of elements obtained from the surface of the microsection showed an increased content of chromium and vanadium in the area of occurrence of primary carbides (**Fig. 3**). The X37CrMoV5-1 steel was characterized by the presence of fine-grained precipitates of alloy carbides in the ferrite matrix with the preserved post-martensitic orientation (**Fig. 4**).

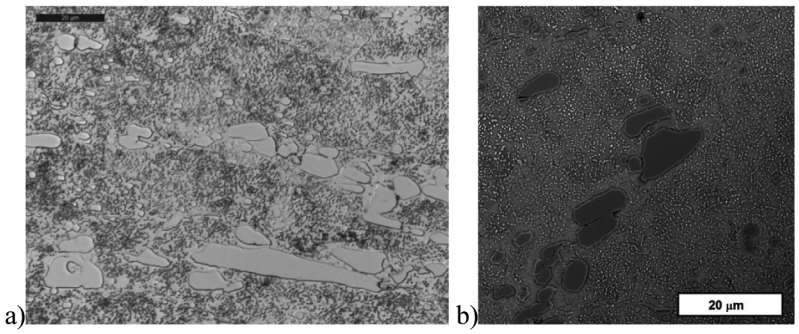

Fig. 2. Microstructure of the X153CrMoV12 cold work steel tested. Visible precipitates of primary carbides against the background of spheroidite. Etched state: a) light microscopy, b) SEM

Rys. 2. Mikrostruktura badanej stali do pracy na zimno gatunku X153CrMoV12. Widoczne wydzielenia węglików pierwotnych na tle sferoidytu. Stan trawiony: a) mikroskopia świetlna, b) SEM

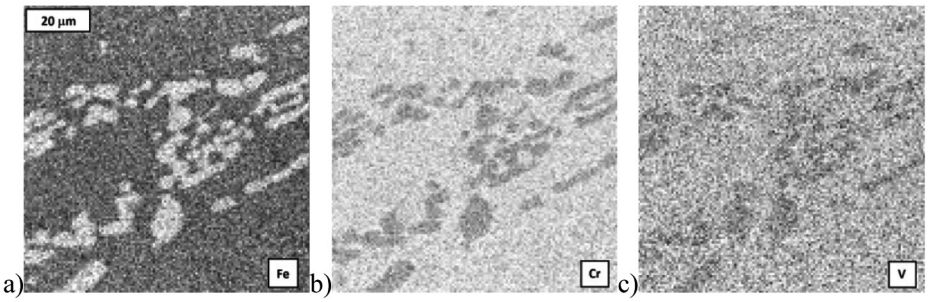

Fig. 3. An example of the distribution of elements Fe (a), Cr (b) and V (c) obtained from the surface of the X153CrMoV12 steel sample. Visible increased content of chromium and vanadium in primary carbides (higher intensity means increased content of element). SEM, EDS

Rys. 3. Przykładowy rozkład Fe (a), Cr (b) oraz V (c) uzyskany z powierzchni próbki ze stali X153CrMoV12. Widoczna zwiększona zawartość chromu i wanadu w węglikach pierwotnych (większa intensywność oznacza zwiększoną zawartość pierwiastka). SEM, EDS

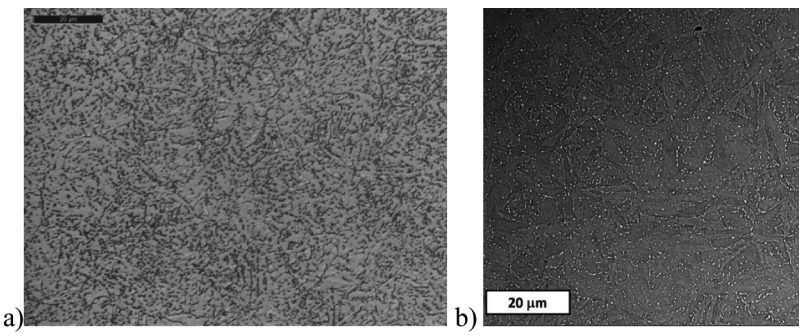

Fig. 4. Microstructure of X37CrMoV5-1 hot work steel tested. High-temperature tempered martensite is visible. Etched state: a) light microscopy, b) SEM

Rys. 4. Mikrostruktura badanej stali do pracy na gorąco gatunku X37CrMoV5-1. Widoczny martenzyt wysokoodpuszczony. Stan trawiony: a) mikroskopia świetlna, b) SEM

Corrosion tests

Analysis of polarization curves obtained in potentiodynamic tests allows assessing the material's corrosion behaviour. The anodic curve is of particular importance in this regard, as it illustrates the corrosive processes taking place. Based on the obtained polarization curves of both alloys, it can be stated that they show similar courses (**Fig. 5**). Their detailed analysis allowed the determination of the electrochemical parameters, which are summarized in **Table 3**. The parameters that are a measure of the corrosion rate, i.e. the corrosion

current $i_{corr,}$ as well as the polarization resistance R_p, are important in this respect. The value of corrosive current obtained using Tafel extrapolation forms the basis for their calculation. The lower the value of i_{corr}, the lower is the rate of corrosion. The polarization resistance is defined as the slope of the polarization curve at low overpotential values (±20 mV) **[L. 17]**. It is associated with the density of the corrosive current and Tafel electrode reaction constants, and it is inversely proportional to the value of the corrosive current. Thus, its higher value indicates a lower intensity of corrosive processes. Both steels tested showed substantially similar values of corrosion currents i_{corr}. However, the X37CrMoV5-1 steel had a lower value of the R_p polarization resistance, which can be related to the lower chromium content in the steel, improving its corrosion resistance. The theoretical chromium content in X153CrMoV12 steel is sufficient to form a passive layer on its surface, analogous to that which ensures high corrosion resistance of austenitic steel. However, it should be noted that, in this case, most of the chromium forms carbides with carbon, so its concentration in the matrix is much lower. The higher silicon content in X37CrMoV5-1 steel should favour its better heat resistance but should not affect the resistance to electrochemical corrosion. Differences were also observed in the case of the corrosion potential E_{corr}. Hot work steel had a slightly lower value of the corrosion potential than the X153CrMoV12 cold work steel.

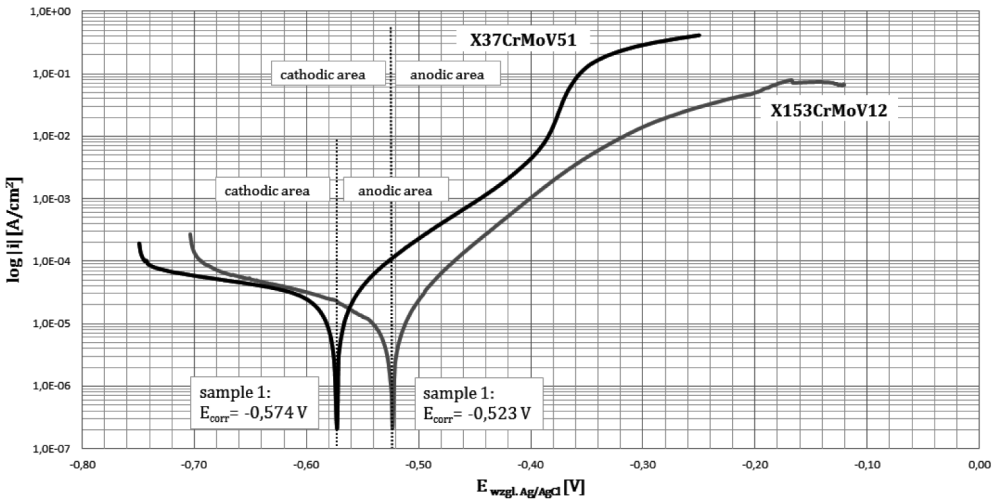

Fig. 5. Exemplary polarization curves obtained during potentiodynamic tests with the corrosion potential value E_{corr} determined for this sample

Rys. 5. Przykładowe krzywe polaryzacyjne uzyskane podczas badań potencjodynamicznych z zaznaczoną wartością potencjału korozyjnego E_{corr} uzyskanego dla badanej próbki

Table 3. Average electrochemical parameters obtained in polarization tests

Tabela 3. Parametry elektrochemiczne uzyskane w badaniach polaryzacyjnych

Steel tested	i_{corr} [μA/cm²]	E_{corr} [mV]	R_p [kΩ]
X153CrMoV12	4.13 ±0.15	-532 ±8.2	2.56 ±0.17
X37CrMoV5-1	5.74 ±0.22	-568 ±9.9	1.24 ±0.19

The mass corrosion rate CR, which was determined in accordance with the standard ASTM G1-90 based on mass losses of both materials subjected to the salt spray test, is also a measure of corrosion intensity. It is defined as the mass change W of the steel proportional to its density D in the exposed surface A and the exposure time t in the corrosion solution analysed. The analysis was based on a relatively short exposure time in the corrosion solution to assess the corrosion rate at the initial stage. The corrosion products formed at this stage on the surface of the alloy inhibit its further development. In the case of the X153CrMoV12 alloy, the value CR = 0.12 mm/year was obtained, while, in the case of the X37CrMoV5-1 alloy, the value CR = 0.13 mm/year was obtained. The parameters used in the calculations are summarized in **Table 4**. The results coincide with the obtained electrochemical parameters.

It should be considered that corrosive wear occurring in tribocorrosion conditions may show different behaviours than in the case when only corrosive wear is analysed. For example, Stachowiak **[L. 1]** showed that austenitic steel shows greater susceptibility

to corrosive-mechanical wear than martensitic steel, despite the commonly known higher corrosion resistance of austenitic steel than martensitic steel. This is due to the lower hardness of this steel, which translates into a greater share of mechanical wear.

Table 4. The parameters used in the calculations of mass corrosion rate CR

Tabela 4. Parametry wykorzystane do wyznaczenia szybkości korozji CR

Steel tested	W [g]	A [cm^2]	D [g/cm^2]
X153CrMoV12	0.046	43.52	7.98
X37CrMoV5-1	0.050	44.33	7.98

Macroscopic and microscopic SEM examination of the surface after electrochemical corrosion tests

Microscopic examination of the surface of samples conducted after electrochemical tests showed that initiated corrosion leads to local changes (**Fig. 5**). Annealing applies to the matrix, while the carbide precipitation occurring in the microstructure remains undamaged (**Figs. 6** and **7**). Such selective destruction of the tool surfaces can contribute to the chipping of the hard carbides made convex in this manner. In the case of high surface pressures, this can lead to chipping off large pieces of material. As shown in **[L. 17]**, different orientation of carbide streaks may contribute to the formation of anisotropy in the intensity of tribological or tribocorrosive wear.

Microscopic observations performed on samples after the testing and removal of corrosion products showed a similar nature of corrosion changes observed on the surface of the samples. The oxidation of the steel matrix was observed, accompanied by the cracking of the surface at the site of oxidation (**Fig. 8**). The resulting cracks are conducive to the spreading of corrosion, because the greater volume of the corrosion products formed there is a "wedging" effect which leads to their further expansion. This reveals a "fresh" surface, which promotes electrolyte penetration and leads to an anode reaction occurring inside the crack. The tops of these cracks will act as micro-anodes and can lead to the propagation of corrosion into the material. The walls of the tunnel and the surface surrounding the crack, in this case, act as a cathode for oxygen reduction.

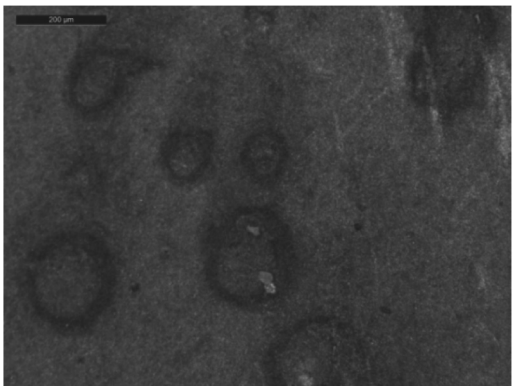

Fig. 6. An example of a microscopic image of the surface of X37CrMoV5-1 steel samples after reaching a potential of approximately +350 mV during the electrochemical tests relative to the corrosion potential. Progressive corrosion is locally visible. Stereoscopic microscopy

Rys. 6. Przykładowy obraz mikroskopowy powierzchni próbek ze stali X37CrMoV5-1 po osiągnięciu podczas badań elektrochemicznych potencjału o wartości około +350 mV względem potencjału korozyjnego. Widoczny lokalny rozwój korozji. Mikroskopia stereoskopowa

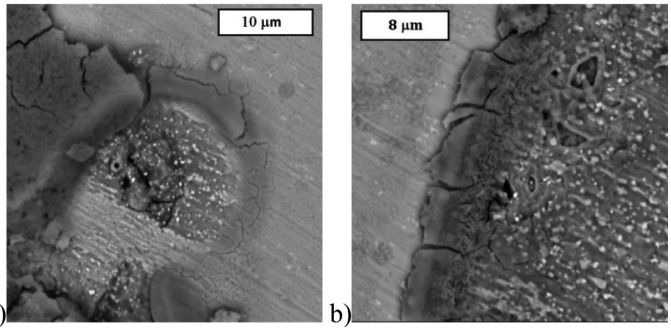

a) b)

Fig. 7. Exemplary microscopic images of the surface of X37CrMoV5-1 steel samples in different areas after reaching a potential of approximately +350 mV during the electrochemical tests relative to the corrosion potential. The matrix dissolution with the unveiling of carbides precipitations is locally visible. SEM

Rys. 7. Przykładowy obraz mikroskopowy SEM powierzchni próbek ze stali X37CrMoV5-1 po osiągnięciu podczas badań elektrochemicznych potencjału o wartości około +350 mV względem potencjału korozyjnego. Widoczne roztwarzanie osnowy z lokalnym odsłonięciem wydzieleń węglikowych. SEM

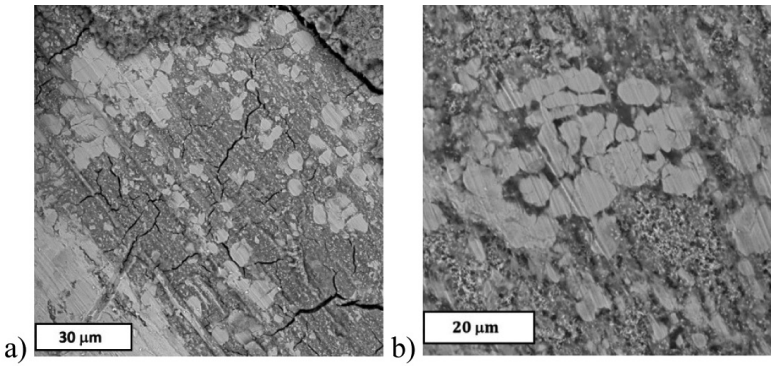

Fig. 8. Exemplary microscopic images of the surface of X153CrMoV12 steel samples in different areas after reaching a potential of approximately +350 mV during the electrochemical tests relative to the corrosion potential. The matrix dissolution with the unveiling of carbides precipitations and cracking of the surface are locally visible. SEM

Rys. 8. Przykładowy obraz mikroskopowy SEM powierzchni próbek ze stali X153CrMoV12 po osiągnięciu podczas badań elektrochemicznych potencjału o wartości około +350 mV względem potencjału korozyjnego. Widoczne roztwarzanie osnowy z ujawnieniem wydzieleń węglikowych i lokalnym pękaniem powierzchni. SEM

Thanks to the tests conducted, we can see that, as a result of the presence of carbide precipitates in the microstructure of tool steels, a micro-cell is formed, the scheme of which is shown in **Fig. 9**. They act as the cathode on which iron ions undergo a reduction reaction. The matrix which acts as the anode is annealed. Fe^{2+} ions combine with OH^-, which leads to the formation of $Fe(OH)_2$. In contact with oxygen dissolved in water, it is then converted into $Fe_2O_3 \cdot nH_2O$, i.e. rust.

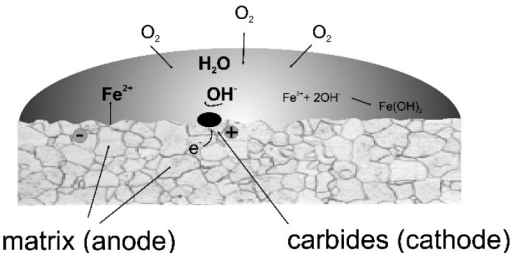

Fig. 9. Scheme of the galvanic cell generated as a result of the presence of carbides in the matrix

Rys. 9. Schemat ogniwa wytworzonego w wyniku obecności węglików w osnowie

Macroscopic and SEM microscopic analysis after salt chamber tests

Both steels tested showed similar character of corrosion changes after the NSS test in a salt chamber (**Fig. 10**). The corrosion products forming on the surface were characterized by an analogous morphological image and chemical composition (**Fig. 11**). Chlorides, present in the spectra of characteristic X-ray radiation, are associated with the use of neutral salt spray tests (**Fig. 12**). Song et al. **[L. 18]** verified that high levels of chloride in corrosive solution led to formation of lepidocrocite γ-FeOOH and β-$Fe_8O_8(OH)_8Cl_{1.35}$ on the carbon steel surface. They observed corrosion products with similar plat-like crystalline morphology of rust layers on metal surface. No other elements were found in the chemical composition of the corrosion products tested.

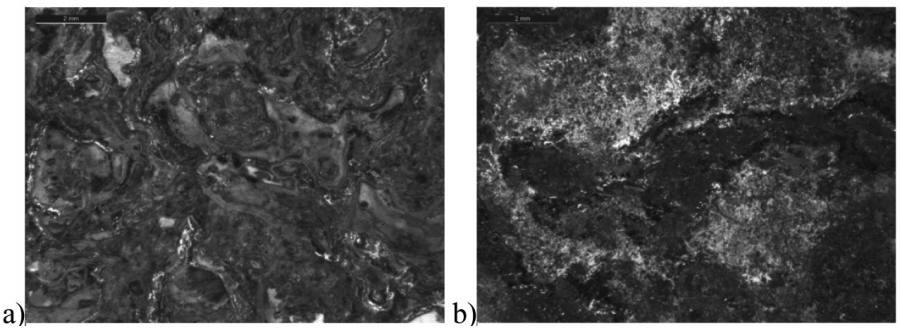

Fig. 10. An example of a stereoscopic image of the surface after 96 hours of the neutral salt spray test (NSS): (a) X153CrMoV12 cold work tool steel, (b) X37CrMoV5-1 hot work tool steel. Stereoscopic microscopy

Rys. 10. Przykładowy obraz stereoskopowy powierzchni po 96 h testu w obojętnej mgle solnej (NSS): (a) stali narzędziowej do pracy na zimno X153CrMoV12, (b) stali narzędziowej do pracy na gorąco X37CrMoV5-1. Mikroskopia stereoskopowa

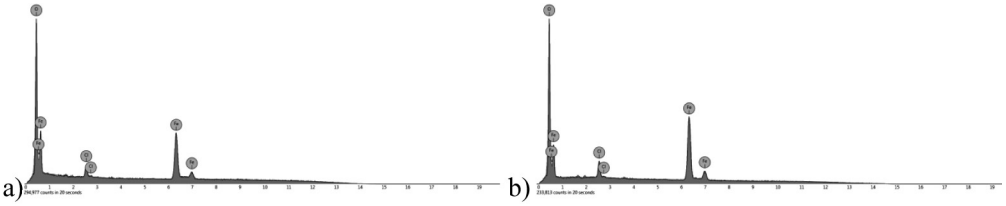

Fig. 11. Corrosion products formed on the surface of the samples after 96 h in neutral salt spray (NSS): a) X153CrMoV12 steel, b) X37CrMoV5-1 steel. SEM

Rys. 11. Produkty korozji powstałe na powierzchni próbek po 96 h testu w obojętnej mgle solnej (NSS): a) stali X153CrMoV12, b) stali X37CrMoV5-1. SEM

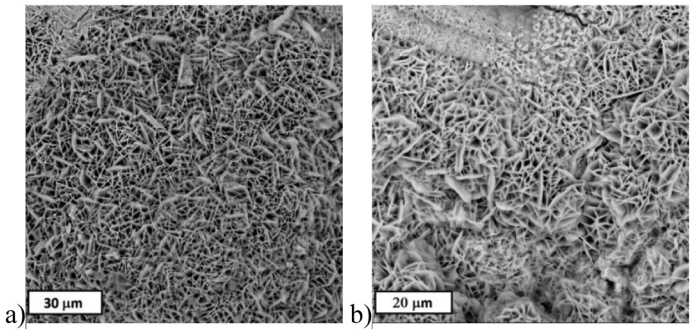

Fig. 12. Characteristic X-ray spectrum obtained from the surface of the samples after the 96 h neutral salt spray test (NSS): a) X153CrMo V12 steel, b) X37CrMoV5-1. SEM, EDS

Rys. 12. Widmo charakterystycznego promieniowania rentgenowskiego uzyskane z powierzchni próbek po 96 h testu w obojętnej mgle solnej (NSS): a) stali X153CrMoV12, b) X37CrMoV5-1. SEM, EDS

SUMMARY

Research on tool wear processes has an important impact on the working lifetime of tools. They are related to the processes taking place at various external interactions, leading to their destruction. In real working conditions, they are the result of the overlap of many elementary wear processes. These include typically tribological wear as well as corrosion related wear. The paper describes the mechanism of corrosive wear of selected tool steels. The role of the microstructure in occurring processes is also discussed. The work assumes that the surface layer of tools undergoes degradation processes caused by thermal processes and leading to changes in the microstructure.

It was found that the tool steels tested exhibit a substantially similar corrosion rates determined by electrochemical tests and NSS tests in a salt chamber. A slightly lower value of the density of corrosion current i_{corr} and CR was found, as well as a higher polarization resistance R_p, indicating better corrosion resistance of X153CrMoV12 grade steel. This steel also had a slightly higher value of corrosion potential E_{corr} than X37CrMoV5-1 grade steel. This can be linked to the higher content of chromium in its chemical composition, which improves steel's resistance to rusting. However, it should be noted that most of the chromium contained in steel is located in carbides, so its content in the matrix is lower than the nominal.

The changes occurring on the surface of tool steels as a result of corrosion processes are local. Active annealing applies to the matrix, while the carbide precipitation occurring in the microstructure remains undamaged. Such selective destruction of the surface contributes to hard carbides becoming convex in such a way, which will be conducive to their chipping and reduce its durability. In the case of high surface pressures, this can lead to chipping off whole pieces of material. The occurrence of a different orientation of carbide streaks may contribute to the occurrence of anisotropy in the intensity of tribological or tribocorrosive wear. A different surface morphology resulting from the corrosion processes will also affect the tribological and working properties of the tools. It should be expected that, under the conditions of tribological impact, occurring corrosion changes have an effect on the values of friction coefficients, wear intensity, and resistance to chipping and flaking of the surface. In particular, this

may promote the formation or intensification of wear by flaking, which is further supported by the high hardness of tool steels.

As corrosion progresses, the process goes deeper into the material, which can change the geometry of the tool. The resulting changes lead to the formation of corrosion micro pitting on the metal surface. This facilitates the increase of stress in the surface layer while the tool is in use. This, in turn, translates into easier initiation and development of microcracks that lead to the formation of fatigue cracks or by spreading, which results in a loss of the cohesion of the metal particle with the surface. As a consequence, material particles may detach from the tool surfaces. Corrosive fatigue cracking may be initiated in the areas of corrosion pits **[L. 10, 19, 20]**. The filling of cracks with corrosion products also hinders the supply of oxygen to them, which promotes the intensification of corrosion as a result of the formation of a concentration microcell.

REFERENCES

1. Stachowiak A.: The identification of corrosive and mechanical wear mechanism in stainless steels in sliding pairs. Problemy Eksploatacji, 2010, nr 1, pp. 83–90 (in Polish).
2. Zwierzycki W., Stachowiak A., Górny K.: Material selection for knife to cutting bell pepper. Tribocorrosion research. Tribologia, 2013, nr 5, pp. 139–148 (in Polish).
3. Beer-Lech K., Surowska B.: Research on resistance to corrosive wear of dental CoCrMo alloy containing post-production strap. Eksploatacja i Niezawodność – Maintenace and Reliability, 2015, Vol. 17 Nr 1, pp. 90–94 (in Polish).
4. Tyczewski P., Nadolny K.: Analysis of mechanical-abrasive-corrosive wear in sugar factories. Inżynieria Rolnicza, 2007, Vol. 93 Nr 5, pp. 409–414 (in Polish).
5. Gauvent M., Rocca E., Meausoone P.J., Brenot P.: Corrosion of Materials Used as Cutting Tools of Wood. Wear, 2006, Vol. 261, pp. 1051–1055.
6. Mohan G.D., Klamecki B.E., The susceptibility of wood-cutting tools to corrosive wear. Wear, 1981, Vol. 74 Issue 1, pp. 85–92.
7. Darmawan W., Rahayu I., Nandika D., Marchal R.: Wear characteristics of wood cutting tools caused by extractive and abrasive materials in some tropical woods. Journal of Tropical Forest Science, 2011, Vol. 23, pp. 345–353.
8. Darmawan W. Rahayu I., Tanaka C., Marchal, R.: Chemical and mechanical wearing of high speed steel and tungsten carbide tools by tropical woods. Journal of Tropical Forest Science, 2006, Vol. 18 No 4, pp. 255–260.
9. Davis J.R: ASM Specialty Handbook: Tool Materials. ASM International, 1995, Materials Park.
10. Wu K., Ito K., Shinozaki I., Chivavibul P., Enoki M.: A Comparative Study of Localized Corrosion and Stress Corrosion Cracking of 13Cr Martensitic Stainless Steel Using Acoustic Emission and X-ray Computed Tomography. *Materials,* 2019, Vol. 12 Issue 16, 2569.
11. Lu S.Y., Yao K.F., Chen Y.B., Wang M.H., Liu X., Ge X.: The effect of tempering temperature on the microstructure and electrochemical properties of a 13 wt.% Cr-type martensitic stainless steel. Electrochimica Acta, 2015, Vol. 165, pp. 45–55.
12. Zhang C., Yamanaka K., Bian H., Chiba A.: Corrosion-resistant carbide-reinforced martensitic steel by Cu modification. Materials Degradation, 2019, Vol. 3, p. 30.
13. Grabke H. J., Spiegel M., Zahs A.: Role of alloying elements and carbides in the chlorine-induced corrosion of steels and alloys. Materials Research, 2004, Vol. *7* No. 1, pp. 89–95.
14. Hrabovský M., Kopřiva M.: Influence of carbides over some steel corrosion. Acta Universitatis Palackianae Olomucensis, Facultas Rerum Naturalium, Physica, 2001-2002, Vol. 40–41 Issue 1, pp. 45–55.
15. Lee J., Lee T., Kwon Y., Mun D.J., Yoo J.Y., Lee C.S.: Role of Mo/V carbides in hydrogen embrittlement of tempered martensitic steel. Corrosion Reviews, 2015, Vol. 33 Issue 6, pp. 433–441.
16. Krawczyk J.: The role of the microstructure in the tribological wear of iron alloys. Wydawnictwo AGH, Kraków 2013 (in Polish).
17. Zybura A., Jaśniok M., Jaśniok T.: Diagnostics of reinforced concrete structures – volume 2. Investigation of reinforcement corrosion and concrete protective properties. PWN, Warszawa 2011 (in Polish).
18. Song Y., Jiang G., Chen Y., Zhao P., Tian Y.: Effects of chloride ions on corrosion of ductile iron and carbon steel in soil environments. Scientific Reports, 2017, Vol. 7, pp. 1–13.
19. Chen G.S., Wan K.C., Gao M., Wei R.P., Flournoy T.H.: Transition from pitting to fatigue crack growth – modeling of corrosion fatigue crack nucleation in a 2024-T3 aluminum alloy, Materials Science and Engineering: A, 1996, Vol. 219 Issues 1–2, pp. 126–132.
20. May M.E., May M., Saintier N., Palin-Luc T., Devos O., Brucelle O.: Modelling of corrosion fatigue crack initiation on martensitic stainless steel in high cycle fatigue regime, Corrosion Science, Elsevier, 2018, 133, pp. 397–405.